NRC Publications Archive
Archives des publications du CNRC

An AC impedance spectroscopy study of freezing phenomena in Wollastonite micro-fibre reinforced cement paste
Sato, T.; Beaudoin, J. J.

Contact us / Contactez nous: nparc.cisti@nrc-cnrc.gc.ca.

National Research Council Canada   Conseil national de recherches Canada

Canada

An AC impedance spectroscopy study of freezing phenomena in wollastonite micro-fibre reinforced cement paste

Sato, T.; Beaudoin, J.J.

National Research Council Canada

Conseil national de recherches Canada

Canada

**An A.C. Impedance Spectroscopy Study of Freezing Phenomena
In Wollastonite Micro-fibre Reinforced Cement Paste**

T. Sato* and J.J. Beaudoin**

***Department of Civil Engineering
University of Ottawa, Ottawa, Ontario
Canada K1N 6N5**

**** Institute for Research in Construction
National Research Council, Ottawa, Ontario
Canada K1A 0R6**

ABSTRACT. A.C. impedance spectroscopy (ACIS) methods were used in studies designed to further understanding of the mechanism of frost action occurring within neat Portland cement paste and cement paste reinforced with wollastonite micro-fibres. An impedance measuring system was coupled with thermomechanical instrumentation to provide real-time impedance spectra and length change data simultaneously on the same specimen during a freezing and thawing cycle. Analysis of the ACIS data provided insight on the relationship between the behavior and mechanism of frost action within the paste systems studied. A mechanistic model (involving interfacial phenomena between liquid water – ice – C-S-H surfaces) based on interpretation of impedance spectra is put forward. In this context the importance of a parameter associated with the depression of the high frequency arc in an impedance spectrum is discussed.

The role of the wollastonite micro-fibre addition in enhancing the durability of cement paste to freezing-thawing is described.

Keywords: Impedance, Cement paste, Wollastonite, Micro-fibres, Freezing

T. Sato is a doctoral student in the Department of Civil Engineering, University of Ottawa. His current research focuses on the synthesis and performance of nanoparticle cement minerals.

J.J. Beaudoin is a Principal Research Officer and Group Leader at the Institute for Research in Construction, National Research Council Canada. His current research activity concerns the application of nanoscience to cement-based materials.

INTRODUCTION

The role of micro-fibres in enhancing the tensile properties of cement-based composite materials has been clearly described by Shah and others [1]. Wollastonite is a natural mineral, calcium meta-silicate (β-CaO–SiO$_2$) and is generally available in the shape of acicular particles for commercial applications. Wollastonite micro-fibres have lateral dimensions of about 25–40 μm and lengths ranging from 0.4–0.6 mm. Improvements in the pre-peak and the post-peak load deflection response by the incorporation of wollastonite micro-fibres occur in Portland cement-based composite systems [2]. The pore structure of these is significantly modified by the addition of wollastonite micro-fibres [3]. Total porosity in the hydrated phases determined by mercury intrusion porosimetry is (in these tests) generally greater than that determined by the helium pycnometry. This suggests that the addition of wollastonite promotes pore discontinuity [4].

The presence of discontinuous pores in the composite system suggests that permeability may be significantly reduced and durability increased. A.C. impedance spectroscopy techniques have been recently used to study the freezing of water in Portland cement paste [5,6]. These techniques were extended to a study of the frost resistance of wollastonite – reinforced cement composites. An assessment of the results is reported.

A.C. IMPEDANCE SPECTROSCOPY

Detection of low temperature phase changes in porous materials using A.C. impedance spectroscopy (ACIS) is a promising new approach to the study of these phenomena. A brief description of the basic elements of impedance spectroscopy is provided [7].

An idealized impedance spectrum for a cement system is plotted in the real versus imaginary plane (Figure 1[a]). A single arc in the high-frequency range and a small part of a second arc in a relatively low-frequency region are shown. The high-frequency arc (HFA) is attributed to the bulk cement paste impedance behavior and the second low frequency arc is due to the cement paste-electrode surface capacitance contribution [8]. The projected intercepts R$_1$ (at the high-frequency end, in the MHz range) and R$_1$ + R$_2$ (at the minimum between the electrode arc and bulk arc, in the kHz range) are important parameters providing information related to cement paste microstructure. Interpretation of an impedance spectrum usually involves modelling with an equivalent circuit (Figure 1[b]) until the electrical response of the elemental microstructure of the cement paste is well simulated.

It is clear that when the frequency approaches an infinite value the projected intercept resistance should be zero. Despite this, extrapolation to the real axis (the dashed line on Figure 1[a]) and computer simulation provide a fictitious or so-called high-frequency resistance which is cement paste microstructure dependent. Work by Gu et al. [9] demonstrated that the high-frequency arc correlates with pore structure parameters and the concentration of ions in the pore solution.
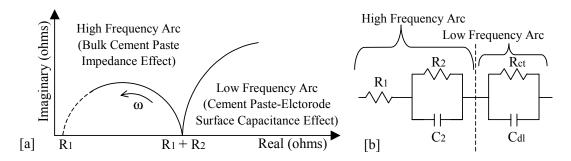
Figure 1   [a] Schematic plot of a high frequency arc in the impedance complex plane obtained for cement paste systems   [b] A simplified electrical equivalent circuit for hydrating system. R_1, R_2 and C_2 are high frequency resistance, solid-liquid interface resistance and capacitance. R_{ct} and C_{dl} are cement-electrode interface charge transfer resistance and double layer capacitance.

In practice, an ideal semi-circle is generally not observed in most materials. It is normally an inclined semi-circle with its centre depressed below the real axis by a finite angle referred to as the depression angle. This behavior, normally associated with a spread of relaxation times [7], cannot be described by the classical Debye equation employing a single relaxation time [10]. A dispersive, frequency-dependent element or so-called constant phase element (CPE) [11,12] can be introduced to account for the shape of the depressed semi-circle. The impedance contribution of this element can be expressed as follows:

$$Z(CPE) = A_0^{-1} \, (j\omega)^{-n} \tag{1}$$

where $n = 1 - (2/\pi) \bullet \theta$ and θ is the depression angle. Therefore, *n* can be used to represent the degree of perfection of the capacitor and represents a measure of how far the arc is depressed below the real impedance axis.

Influencing factors on the depression angle such as a spread of relaxation times and non-Debye behavior have been suggested [7]. A wider spread of pore diameters can also be associated with a larger depression angle [11]. The time for the reorientation of ions or relaxation time appears to be affected by the geometry of the pores and the surface chemistry of the solid. A stronger ion-ion interaction would be expected in small pores. A broader pore size distribution would result in a wide spread of relaxation times corresponding to a larger depression angle. Distributed circuit elements are often associated with microscopic characteristics such as interface properties and grain boundary effects. It would therefore be expected that formation of ice in pores would affect the extent to which interfaces influence impedance behavior.

EXPERIMENTAL

Materials

A type 10 normal Portland cement was used as the binding material. The wollastonite micro-fibres were 25–30 μm in the transverse dimension and 0.4–0.6 mm in length.

Specimen Preparation

The cement paste composite specimens were prepared at water-cement (w/c) ratios of 0.35, 0.40, 0.50 and 0.60 and were hydrated for 1, 3, 7 and 28 days. The wollastonite contents were 0, 5.1, 8.1 and 10.2 percent by volume.

The composite specimens were cylindrical, 9.64 mm in diameter and 19.05 mm in length. Two stainless steel electrodes to which electric wires were soldered were cast into the end of each specimen. The specimens prepared at w/c ratio 0.60 were hydrated by rotating molds for the first 24 h to minimize bleeding. All specimens were demolded the day following casting. They were then wet-cured in saturated calcium hydroxide solution for the desired hydration period.

Apparatus

The equipment used to measure the ACIS response of the samples was the 1260 Solarton Gain-Phase Analyser. This apparatus was controlled by the computer software Z60.

The DuPont Thermomechanical Analyser 2940 (TMA) apparatus was used to control the temperature variations as well as to measure the changes in length of the specimen. Liquid nitrogen was kept in the cold finger that lowered to enclose the specimen. The apparatus is equipped with a furnace to control the temperature variations at the desired rates.

The apparatus used to conduct the Differential Scanning Calorimetry (DSC) and Thermogravimetric Analysis (TGA) tests were the DuPont 2910 and 951 analysers, respectively. The DSC was used to estimate the amounts of frozen water and, TGA, the degree of hydration.

Testing Procedure

The test specimens were inserted into the TMA apparatus in a saturated surface dry condition. The wires connected to the electrodes were carefully placed so that they would extend outside the cold finger and yet would not interfere with it. The following outlines the temperature regime used for each test:
1. Isothermal conditions at +5°C were held for 10 min. Impedance measurements were started at the beginning of the isothermal segment.
2. The temperature was decreased at a rate of 2°C/min to a minimum of −80°C.
3. Isothermal conditions at −80°C were held for 10 min.
4. The temperature was increased at the rate of 2°C/min to a maximum of +20°C.
5. Isothermal conditions at +20°C were held for 5 min.

The raw data collected by the Solarton 1260 Gain-Phase Analyser were then fit to an equivalent circuit using the Zview software. Each impedance spectrum was fit to a corresponding equivalent circuit from which the sample resistance and depression angle parameter were obtained. For each test, more than 100 impedance spectra were recorded and their corresponding equivalent circuits determined.

RESULTS AND DISCUSSION

The paper is concerned with the electrical measurements. Changes to the impedance spectra in terms of the resistance values and the depression angle parameter, n, are of primary interest. A discussion of the characteristics of the high frequency arc for non-reinforced cement paste in terms of interfacial phenomena existing at low temperature is useful in order to assess the influence of wollastonite micro-fibres on freezing-thawing resistance. This follows.

Analysis of Low Temperature Impedance Spectra

The high frequency arc

The high frequency arc can be modelled by using the mathematical expression of the equivalent circuit in Figure 1[b].

$$Z = R_1 + \left(\frac{1}{1/R_2 + j\omega C_2} \right) \tag{2}$$

Xie et al. [8] described R_1 as the resistance of the pore water and R_2 and C_2 as the resistance and capacitance of the C-S-H and pore water interface of cement paste at room temperature, respectively. The interpretation of phenomena associated with these three parameters can be aided with reference to Figure 2[a]. Consider a cement paste subjected to a freezing process. Subsequent to freezing and the ice formation (Figure 2[b]), the C-S-H and pore water interface becomes the combination of the C-S-H and pore water interface and the C-S-H and ice interface. It follows that as the values of R_2 and C_2 of the C-S-H and ice interface are much greater than those of the C-S-H and pore water interface; the values of R_2 and C_2 represent the resistance and capacitance of the C-S-H and ice interface. The value of R_1 is not affected by the C-S-H and pore water interface or the C-S-H and ice interface. The significance of interfacial effects will be discussed later with reference to the depression angle parameter as a durability indicator.
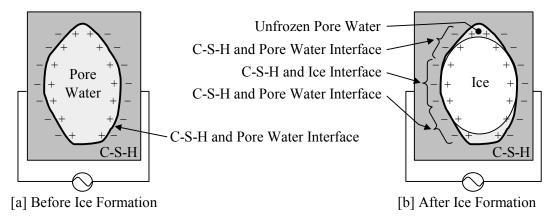

[a] Before Ice Formation   [b] After Ice Formation

Figure 2   Modelling impedance spectra for cement paste subjected to a freezing and thawing cycle.

The resistance ratio, λ_R

The resistance R_2 is the resistance of the C-S-H and pore water interface of cement paste before ice formation and the resistance of the C-S-H and ice interface after ice formation. Figure 3 is a plot of resistance R_2, on a logarithmic scale, versus temperature for a cement paste specimen of w/c ratio 0.50 at 7 days hydration subjected to a freezing and thawing cycle. The value of R_2 increases as soon as the temperature starts decreasing even before ice formation occurs. Its rate of change increases when ice formation is initiated at $-7°C$. Then the value of R_2 continues to increase semi-logarithmically. As the interfacial area of the C-S-H and pore water changes to that of the C-S-H and ice, its resistance increases. The slope of the curve in Figure 3 between $5°C$ and $-7°C$ and the curve between $-65°C$ and $-80°C$ on freezing are approximately equal, indicating that the freezing of the water is essentially complete at $-65°C$. A resistance ratio, λ_R, can then be introduced as follows:

$$\lambda_R = R_f / R_i \qquad\qquad (3)$$

where λ_R = resistance ratio
        R_f = resistance at completion of freezing of pore water, Ω
        R_i = resistance at beginning of freezing of pore water, Ω

The amount of freezable water obtained from DSC analysis can be correlated to the resistance R_2. The value of λ_R therefore provides an index of both the amount of resistance increase, and the amount of freezable water. The resistance ratio is therefore related to the durability of cement paste. This relation will be discussed later.
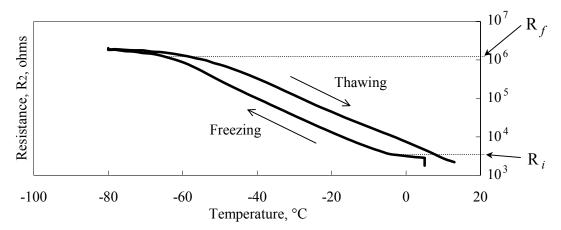

Figure 3   Resistance, R_2, versus temperature for a cement paste specimen, w/c ratio 0.50, at 7 days hydration subjected to a freezing and thawing cycle

The depression angle parameter, n

The depression angle parameter provides valuable information to further understanding of the complex mechanism of frost action. It is suggested that the depression angle parameter is dependent on interface characteristics such as heterogeneity and roughness. It decreases as

the interface becomes more heterogeneous and rough. Conversely, as the interface becomes less heterogeneous and rough, the depression angle parameter approaches 1.00.

Figure 4 is a plot of the depression angle parameter versus temperature for a cement paste specimen of w/c ratio 0.50 at 7 days hydration subjected to a freezing and thawing cycle. The depression angle parameter starts with a value of approximately 0.953 at 5°C and decreases to 0.945 as the temperature decreases to –25°C. It then increases to about 1.00 as the temperature decreases to –80°C. The changes associated with the temperature variation can be explained by the heterogeneity of the interface. Let us consider the "C-S-H interface" at 5°C, as the C-S-H and pore water interface (Figure 2[a]). The "C-S-H interface" is said to be homogeneous. Ice formation in the capillary pores transforms the "C-S-H interface" into a combination of the C-S-H and pore water interface and the C-S-H and ice interface. The "C-S-H interface" is now considered heterogeneous (Figure 2[b]).

The depression angle parameter decreases as the temperature is lowered (Figure 4) since the "C-S-H interface" becomes more heterogeneous as some ice formation takes place. At approximately –25°C, the depression angle parameter starts to increase. When the C-S-H and ice interface occupies about 0 to approximately 50 percent of the "C-S-H interface", the increase of the C-S-H and ice interface results in a more heterogeneous "C-S-H interface". The increase of the C-S-H and ice interface beyond 50 percent at results in a more homogeneous "C-S-H interface" and an increase of the depression angle parameter.
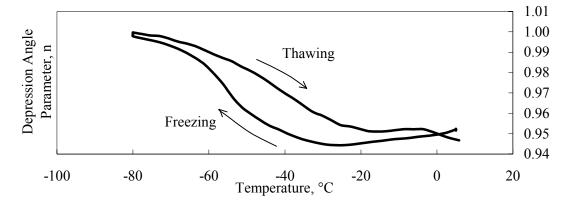

Figure 4   Depression angle parameter, n, versus temperature for a cement paste specimen, w/c ratio 0.50, at 7 days hydration subjected to a freezing and thawing cycle

The depression angle parameter continues to increase to approximately 1.00 as the C-S-H and ice interface occupies a greater proportion of the "C-S-H interface". However, there is a difference in the values between the depression angle parameter at 5°C and at –80°C. The depression angle parameter affected by the pores fully occupied by the C-S-H and pore water interface (5°C) and fully occupied by the C-S-H and ice interface (–80ºC) should be approximately equal in terms of heterogeneity of the interface. However, the value of the depression angle parameter at 5°C is about 0.95, while the value at –80°C is close to 1.00. The reason may be related to the roughness of "C-S-H interface". This concept is described with the aid of the models illustrated in Figure 5. The C-S-H consists of small gel particles

which may create a rough surface along the wall of the capillary pore, Figure 5[a]. The "C-S-H interface" becomes less rough when the water in the capillary pore freezes (Figure 5[b]). This results in an increase in the depression angle parameter. Furthermore, when the freezing takes place in the gel pores, it causes the surface of the small C-S-H particles to become less rough.

This leads to a further increase in the depression angle parameter. This explanation is compatible with observed behavior in the temperature range 5 to –25°C. In this range the "C-S-H interface" becomes less rough as soon as ice formation starts. However, the depression angle parameter decreases because the effect of the heterogeneity of the "C-S-H interface" is more dominant than that of the roughness of the "C-S-H interface". The "C-S-H interface" becomes less heterogeneous and rough when the temperature falls below –25°C. This results in the higher depression angle parameter at –80°C than the one at 5°C.
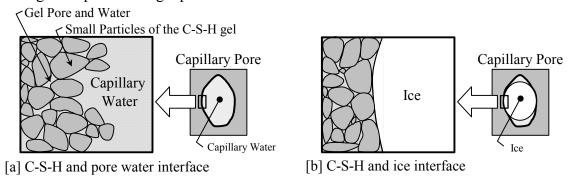

[a] C-S-H and pore water interface   [b] C-S-H and ice interface

Figure 5   Models of the "C-S-H interface" in a capillary pore illustrating the concept of interface roughness

Effect of Wollastonite Content

Resistance ratio, λ_R

The resistance ratio, λ_R corresponds to the amount of freezable water in the cement composite system. λ_R was calculated as a function of wollastonite content for cement composites prepared at various w/c ratios hydrated 28 days. The addition of wollastonite micro-fibres is only effective when the content exceeds 10 percent by volume. The improvement at this content is 2.9, 21.2, 34.8 and 23.1 percent for w/c ratio 0.35, 0.40, 0.50 and 0.60 respectively. The amount of water frozen in the paste binder containing 10.2 percent wollastonite by volume is significantly lower than for plain cement pastes. This is not the case for pastes with other micro-fibre contents. It would appear that not all the porosity is saturated (at 28 days hydration) when the cement composite contains greater than 10 percent wollastonite. The improved resistance ratio corresponds well to a lower amount of ice.

The depression angle parameter, n

The effect of wollastonite micro-fibre reinforcement on the value of n at 1 and 28 days is illustrated in Figure 6. The character of the depression angle parameter curves are indicative of the factors that affect mass transfer of water due to phase changes associated with ice

nucleation and growth. The initial decrease of n at 1 day hydration suggests that mass transfer is not strongly impeded by the boundary conditions at the surface – both electrical and physical. Ice formation subsequently minimizes the effect of surface charge at the expense of surface roughness as the ice content increases physical resistance to mass transfer. The dynamic interplay between the surface charge and the physical resistance determines the rate and direction of the depression angle parameter, n. The description of surface homogeneity given earlier relates to the degree of surface charge modification due to ice formation.
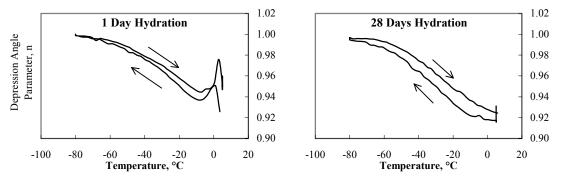

Figure 6   Depression angle parameter, n, versus temperature for the cement paste specimens, w/c ratio 0.40, containing 10.2% wollastonite content at 1 and 28 days hydration

Cement paste porosity is decreased as hydration proceeds. The pore surface exposed to liquid water molecules is reduced. Physical restrictions to flow increase as surface effects on the impedance response diminish. There is a transition in liquid containing pore space which is analogous to a dynamic change in pore structure. The wollastonite content does not appear to significantly affect the shape of the curves (at a specific w/c ratio and degree of hydration) suggesting that the presence of the micro-fibres does not significantly affect the mass transfer process itself as a result of a cooling-warming cycle. This would further suggest that improvement in freezing-thawing resistance is due to the reinforcing effect of the fibres themselves in addition to the lower amount of freezable water in the binder.

CONCLUSIONS

1. Low temperature impedance spectra provide useful information for studies of freezing-thawing phenomena in microporous materials.
2. The ratio of resistance values at the completion and initiation of the water-ice transition has value as a durability index. Its magnitude corresponds to the amount of freezable water in the system.
3. A parameter related to the depression angle of the high frequency arc in an impedance spectrum provides information related to the nature of mass transport below the triple point in a water saturated microporous medium.
4. Wollastonite micro-fibre reinforcement of cement binders appears to improve resistance to a freezing-thawing cycle up to 35 percent when present in amounts exceeding 10 percent by volume.

5. The presence of wollastonite micro-fibres in a cement paste matrix does not appear to significantly affect the mass transfer process itself as a result of a cooling-warming cycle. Improvement in freezing-thawing resistance is likely due to the reinforcing effect of the fibres in addition to the amount of freezable water in the binder.

ACKNOWLEDGMENTS

REFERENCES

1. BETTERMAN, L.R., OUYANG, C., SHAH, S.P., Fiber-matrix interaction in microfiber-reinforced mortar, Advanced Cement Based Materials, 2, 1995, pp 53-61
2. LOW, N.M.P., BEAUDOIN, J.J., Flexural strength and microstructure of cement binders reinforced with wollastonite micro-fibers, Cement Concrete Research, 23, 1993, pp 905-916
3. LOW, N.M.P., BEAUDOIN, J.J., The effect of wollastonite micro-fibre aspect ratio on reinforcement of Portland cement-based binders, Cement Concrete Research, 23, 1993, pp 1467-1479
4. BEAUDOIN, J.J., Porosity measurements of some hydrated cementitious systems by high pressure mercury porosimetry-microstructural limitations, Cement Concrete Research, 9, 1979, pp 771-781
5. PERRON, S., BEAUDOIN, J.J., Freezing of water in Portland cement paste – An a.c. impedance spectroscopy study, Cement Concrete Composites, 24, 2002, pp 467-475
6. OLSON, R.A., CHRISTENSEN, B.J., COVERDALE, R.T., FORD, S.J., MOSS, G.M., JENNINGS, H.M., Interpretation of the impedance spectroscopy of cement paste via computer modeling, Part III Microstructural analysis of frozen cement paste, Journal of Materials Science, 30, 1995, pp 5078-5086
7. McCARTER, W.J., GARVIN, S., BOUZID, N., Impedance measurements on cement paste, Journal Materials Science Letters, 7, 1988, pp 1056-1057
8. XIE, P., GU, P., XU, Z., BEAUDOIN, J.J., A rationalized a.c. impedance model for microstructural characterization of hydrating cement systems, Cement Concrete Research, 23, 1993, pp 359-367
9. GU, P., XU, Z., XIE, P., BEAUDOIN, J.J., LOW, N.M.P., Impedance studies of wollastonite micro-fibre reinforced cement paste systems, Advances in Cement Research, 5, 1993, pp 87-92
10. MacDONALD, J.R., JOHNSON, W.B., Impedance Spectroscopy, J. Wiley & Sons, New York, 1987, p 346
11. SLUYTERS-REHBACH, M., SLUYTERS, J.H., Electroanalytical Chemistry, Marcel Dekker, New York, 1990, p 329
12. COLE, K.S., COLE, R.H., Dispersion and absorption in dielectrics I. Alternating current characteristics, Journal of Chemical Physics, 9, 1941, pp 341-351